# Green Synthesis and Characterization of Ni-Cu-Mg Ferrite Nanoparticles in the Presence of Tragacanth Gum and Study of Their Catalytic Activity in the Synthesis of Hexanitrohexaazaisowurtzitane

***Taghavi Fardood, Saeid; Ebadzadeh, Behrooz; Ramazani, Ali****[+]

*Department of Chemistry, University of Zanjan, Zanjan, I.R. IRAN*

**ABSTRACT:** *Here, we report the synthesis, characterization and catalytic evaluation of Ni-Cu-Mg ferrite using tragacanth gum as biotemplate and Metals nitrate as the metal source by the sol-gel method without using any organic chemicals. The sample was characterized by powder X-Ray Diffraction (XRD), Fourier Transform Infrared Spectroscopy (FT-IR), Vibrating Sample Magnetometer (VSM) and Scanning Electron Microscopy (SEM). The X-Ray powder Diffraction (XRD) analysis revealed the formation of cubic phase ferrite MNPs with an average crystallite size of 19 nm. Magnetic analysis revealed that the Ni-Cu-Mg ferrite nanoparticles had a ferromagnetic behavior at room temperature with a saturation magnetization of 27.85 emu/g. The catalytic activity of Ni-Cu-Mg ferrite MNPs was evaluated for the synthesis of 2,4,6,8,10,12-hexabenzyl-2,4,6,8,10,12-hexaazatetracyclo [5.5.0.05,9.03,11 ] dodecane (HBIW) under ultrasonic irradiation. The catalyst could easily be recycled and reused few times without noticeable decrease in catalytic activity.*

**KEYWORDS:** *Ferrites; Tragacanth gum; Natural Hydrogel; HBIW; Ultrasonic irradiation*.

## INTRODUCTION

In the last decade, nanostructured materials have long been considered as new properties such as magnetic, electronic, catalysis, energy science, optoelectronics, photo-electrochemical, biomedical sciences, energy science, mechanical, and optical materials in nano dimensions that these properties cannot be observed in bulk [1-11]. Nowadays, The use of magnetic nanoparticles as a catalyst taken into consideration because of their advantages such as green, low-cost, efficient, magnetic properties and reusable catalysts [12-16]. The properties of ferrites can be improved by substitutions or additions, and also by controlling the sintering temperature and time [17,18]. The current tendency is focused on doped ferrite materials prepared *via* numerous synthesization techniques with several cation concentrations that in turn affect the various properties such as electrical, dielectric, and magnetic. Ni–Cu–Mg ferrites are used as standard soft magnetic materials for multilayer ferrite inductors because of their low sintering temperature and full performance up to MHz frequencies. Correlations among the composition of Ni–Cu–Mg ferrites and their sintering performance and magnetic properties have been studied [19-21].

***** *To whom correspondence should be addressed.*

*+ E-mail: aliramazani@gmail.com*

*1021-9986/2019/6/21-29* *9/$/5.09*

Since the defense industry is a model for development in various industries, a possible way to execute this progress consists of the designing of highly energetic compounds that provide the explosion power superior to any existing substance. Cage crystal molecules containing the nitro groups are important and widely used as high energetic materials that much attention have attracted in the last ten years [22,23]. According to the theoretical predictions on the physicochemical and explosion characteristics, polycyclic nitramines, in particular, hexanitrohexaazaisowurtzitane, HNIW, CL-20, is a unique representative of this class of compounds [24-26]. Hexabenzylhexaazaisowurtzitane (HBIW) is used as a precursor for the synthesis of HNIW. The only available method for the construction of the HBIW cage is based on the condensation of glyoxal with benzylamine in the presence of formic acid as a catalyst [27,28]. This method is efficient; however, the catalyst recovery/reuse is not possible. Therefore, the introduction of efficient procedures with easily separable and reusable catalysts for the preparation HBIW is needed. For this purpose use of magnetically catalysts like Ni-Cu-Mg ferrite has received considerable attention as remarkable catalytic activity, easy synthesis, nontoxic, reusability, economic viability, ecofriendliness, and recoverability encouraged us to utilize it as a catalyst for the synthesis of HBIW. Gums are naturally occurring polysaccharide components in plants, which are mostly green, economical, and easily available. Tragacanth Gum (TG) is a naturally occurring complex, an acidic polysaccharide derived as an exudate from the bark of Astragalus gummifer (Fabaceae family), a native tree of western Asia. It is commercially produced mostly in Iran and Turkey [29,30,13]. In this work, we have synthesis Ni-Cu-Mg ferrite nanoparticles using TG by the sol-gel method as a cheap, facile and friendly approach to the nature. The catalytic activity of Ni-Cu-Mg ferrite nanoparticles has been evaluated for the synthesis of HBIW with a facility and appropriate method under eco-friendly conditions, as shown in Scheme 1.

In the phenomenon of reductive hydrogenolysis (acetyl debenzylation) of HBIW, one of the intermediate products (polyacetylpolybenzyl derivative) was TADBIW. Best yields were obtained by catalytic hydrogenolysis using palladium hydroxide on carbon with acetic anhydride solvent along with the acid promoter like HBr under atmospheric pressure of hydrogen [31]. The chemical representation of the synthesis of HNIW through HBIW is given in Scheme 2.

## EXPERIMENTAL SECTION

### *General Information*

The Tragacanth Gum (TG) was obtained from a local health food store.

All the chemicals were purchased from Fluka AG, Merck, daijung (Darmstadt, Korea) Aldrich and were used without further purification. The reactions were monitored by TLC. Sonication was performed in a Bandelin (Berlin, Germany) SONOPULS ultrasonic homogenizers with 20-kHz processing frequency, a nominal power of 250 W, and uniform sonic waves. Melting points were measured with an Electrothermal 9100 apparatus (LABEQUIP LTD., Markham, Ontario, Canada) and are uncorrected. $^{1}H$ (DMSO-$d_6$) and $^{13}C$ NMR (DMSO-$d_6$) spectra were recorded on a Bruker DRX-250 Avance spectrometer at 250.13 and 62.90 MHz, respectively.

The structural properties of $NiCuMgFe_2O_4$ MNPs were analyzed by X-Ray Powder Diffraction (XRD) with a X'Pert-PRO advanced diffractometer using Cu (Kα) radiation (wavelength: 1.5406 Å), operated at 40 KV and 40 MA at room temperature in the range of 2θ from 20 to 70. InfraRed spectra were recorded on a Mattson (Unicam Ltd., Cambridge, UK) 1000 Fourier transform infrared spectrophotometer using KBr technique. The particle size and morphology of the sample surfaces was studied by a Scanning Electron Microscope (Zeiss EVO 18). The magnetic properties of the sample was detected at room temperature using vibrating sample magnetometer (VSM, Meghnatis Kavir Kashan Co., Kashan, Iran).

### *Preparation of $Ni_{0.35}Cu_{0.25}Mg_{0.4}Fe_2O_4$ MNPs*

To prepare $Ni_{0.35}Cu_{0.25}Mg_{0.4}Fe_2O_4$ MNPs, Ni $(NO_3)_2.6H_2O$, Cu $(NO_3)_2.3H_2O$, Mg $(NO_3)_2.6H_2O$, and Fe $(NO_3)_3.9H_2O$ were used as starting materials. Firstly, 0.2 g of the Tragacanth Gum (TG) was dissolved in 40 mL of deionized water and stirred for 80 min at 70 ºC to achieve a clear Tragacanth Gel (TG) solution. After that, the stoichiometric mixtures of the mentioned materials were added to the TG solution and, the container was moved to a sand bath. The temperature of the sand bath was fixed at 75 ºC and stirring was continued for 12 h to obtain a brown color resin. The final product was calcined at 700 ºC in air for 4h to obtain $Ni_{0.35}Cu_{0.25}Mg_{0.4}Fe_2O_4$ MNPs.

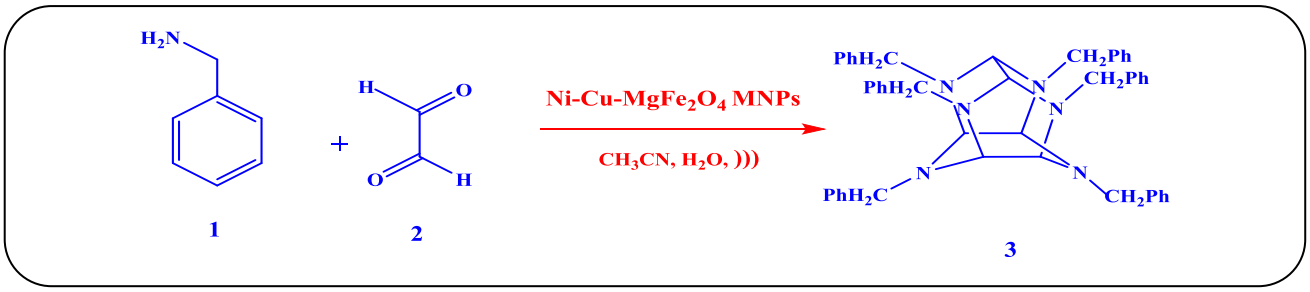


***Scheme 1: Synthesis of HBIW in the presence of Ni-Cu-MgFe$_2$O$_4$ MNPs.***

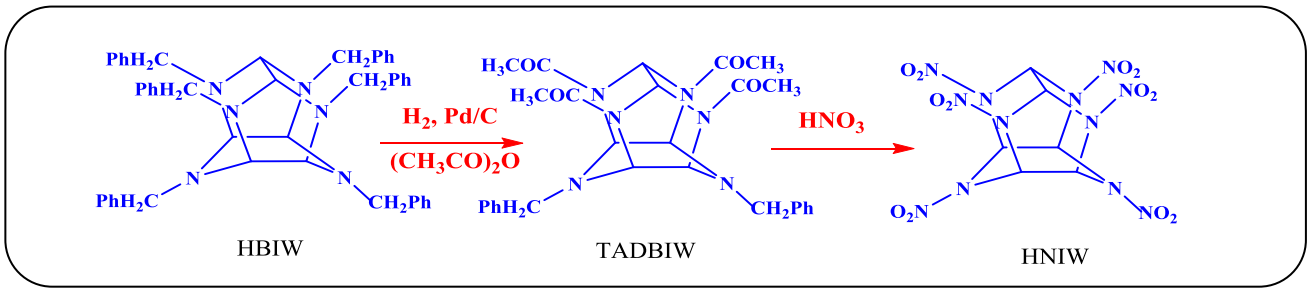


***Scheme 2: Synthesis of HNIW from HBIW.***

***Typical procedure for synthesis of HBIW***

Benzylamine (0.0085 mol, 0.937 mL), NiCuMgFe$_2$O$_4$ MNPs (10% mol with respect to glyoxal), acetonitrile (7.75 mL), and water (0.775 mL) was placed in a round-bottomed flask of 100 mL. The reaction mixture was stirred at room temperature and glyoxal (40% aqueous solution; 0.00375 mol, 0.427 mL) was added dropwise (15 min). Then the mixture was irradiated with ultrasound under a power of 150W for 5 min. Formation of HBIW monitored by TLC. After the completion of the reaction, the NiCuMgFe$_2$O$_4$ MNPs were removed by an external magnet. The precipitate was collected by simple paper filtration and purified via recrystallization from ethanol. For further purification can use of ethyl acetate. The reaction yield is 91% based on the obtained recrystallized product.

***Data Spectra of Product***

White solid; m.p.: 155–157 ºC.

FT-IR (KBr): 3022, 2942, 2835, 1951, 1601, 1450, 1351, 1169, 1138, 989, 926, 836, 732, 699. $^1$HNMR ($CDCl_3$) $\delta_H$: 7.24–7.28 (m, 30H, phenyl CH), 4.16 (s, 4H, $CH_2$), 409 (s, 8H, $CH_2$), 4.04 (s, 4H, CH), 3.57 (s, 2H, CH). $^{13}$CNMR ($CDCl_3$): 56.21-56.88 (6C, $CH_2$-phenyl), 76.51-80.64 (6C, CH (skeletal), 126.62-140.74 (36C, phenyl).

## RESULTS AND DISCUSSION

***Catalyst characterization***

FT-IR spectra were recorded in solid phase using the KBr pellet technique in the range of 400-4000 cm$^{-1}$. Fig. 1 shows the IR spectrum of the sample calcined at 700°C for 4 hours. According to Fig. 1, two strong absorption bands $\nu_1$ and $\nu_2$ are observed at 586 cm$^{-1}$ and 425 cm$^{-1}$, respectively. The difference between $\nu_1$ and $\nu_2$ is due to the changes in bond length (Fe-O) at the octahedral and tetrahedral sites. The bands at 3418 cm$^{-1}$ and 1634 cm$^{-1}$ are characteristic for hydroxyl group (O-H). The peaks at 1435 cm$^{-1}$ and 1017 cm$^{-1}$ may be ascribed to C-O and -C-O-C stretching modes [32].

The crystal structure confirmation analysis was carried out by the X-ray diffraction patterns. XRD pattern of the product obtained by calcination of the precursor at 700 °C is shown in Fig. 2.

XRD analysis showed a series of diffraction peaks at 2θ of 30.37, 35.64, 37.22, 43.25, 53.65, 56.75 and 62.88 could be assigned to (220), (311), (222), (400), (422), (511) and (440) planes, respectively. All the diffraction peaks were readily indexed to a pure cubic structure ferrite (JCPDS Card no. 44-1485) with a=b =c= 8.354 Å. No diffraction peaks of other impurities were observed. The average particle size of ferrite nanoparticles was determined from the Full Width at Half Maximum (FWHM)

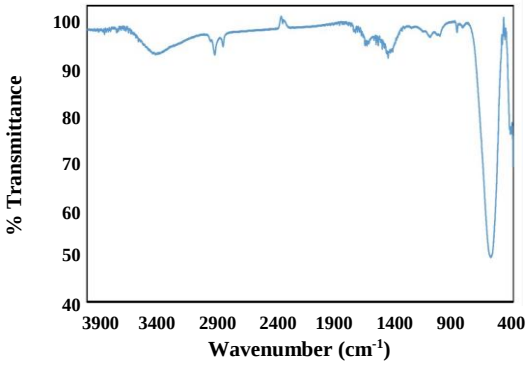


*Fig. 1: FT-IR spectrum of $Ni0_{.35}Cu_{0.25}Mg_{0.4}Fe_2O_4$ MNPs calcined in air at 700 ºC for 4 h.*

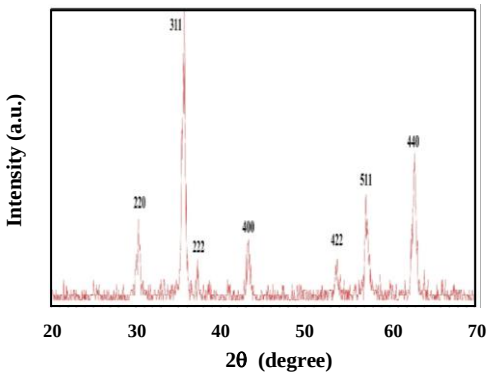


*Fig. 2: XRD pattern of $Ni_{0.35}Cu_{0.25}Mg_{0.4}Fe_2O_4$ MNPs calcined in air at 700 ºC for 4 h.*

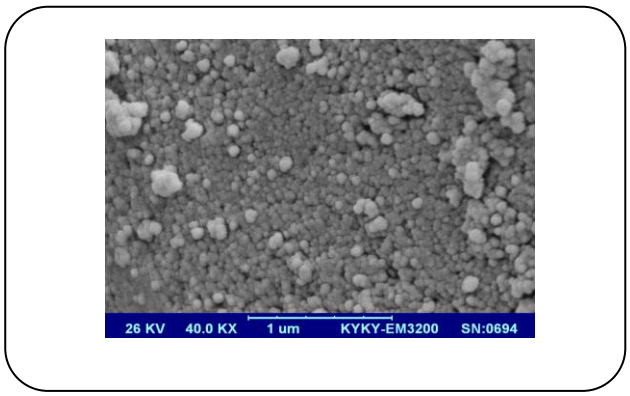


*Fig. 3: SEM micrograph of the $Ni_{0.35}Cu_{0.25}Mg_{0.4}Fe_2O_4$ MNPs calcined in air at 700 ºC for 4 h.*

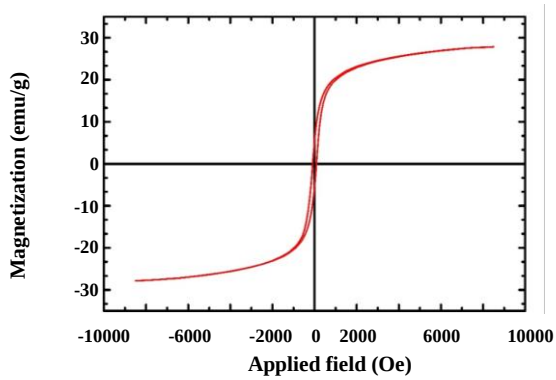


*Fig. 4: Magnetization curve of $Ni_{0.35}Cu_{0.25}Mg_{0.4}Fe_2O_4$ MNPs calcined in air at 700 ºC for 4 h.*

of the XRD patterns using the well- known Scherrer formula: $D = 0.9\lambda/\beta\cos\theta$

Where D is the crystallite size (nm), β is the full width at half maximum of the peak, λ is the X-ray wavelength of Cu Kα= 0.154 nm and θ is the Bragg angle [33]. Using the above method we obtained an average crystallite size of 19 nm for $Ni_{0.35}Cu_{0.25}Mg_{0.4}Fe_2O_4$ MNPs.

The SEM image shows the particle size and external morphology of the ferrite nanoparticles that calcined at 700 ºC for 4h (Fig. 3). It can be seen from the SEM image, the ferrite nanoparticles have fairly uniform spherical shape and narrow size distributions.

To study the magnetic behavior of $Ni_{0.35}Cu_{0.25}Mg_{0.4}Fe_2O_4$-NPs, magnetization measurements recorded with VSM were performed. As can be observed in Fig. 4, the specific saturation magnetization value was measured to be 27.85 emu/g for $Ni_{0.35}Cu_{0.25}Mg_{0.4}Fe_2O_4$-NPs. Remanence magnetization (Mr) and coercivity (Hc) values of the $Ni_{0.35}Cu_{0.25}Mg_{0.4}Fe_2O_4$-NPs calcined at 700 °C are 89.35 Oe and 3.32 emu/g, respectively. The sample exhibited a magnetic property in the presence of a magnetic field.

The prepared Ni-Cu-$MgFe_2O_4$ MNPs was investigated as a catalyst in the synthesis of HBIW under ultrasonic irradiation. We optimized the reaction conditions such as catalyst amount, ultrasonic power, type of solvent and reaction times.

### *Effect of amount catalyst on product yield*

In order to verify the effect of catalyst on product yield, the reaction between benzylamine and glyoxal was done under different catalytic conditions. As shown in Table 1, the optimum yield of the product was obtained when 10 mol % of catalyst was used. It was found that in the absence of a catalyst, the product was obtained in 14% yield within 5 min.

### *Effect of various solvent on the product yield*

The effect of solvent on the yield of HBIW is given in Table 2. In these experiments, we observed that

***Table 1: Effect of the amount of catalyst in the synthesis of HBIW.***

| Entry | Catalyst (mol%) | ultrasonic power (W) | Time (min) | Yield (%)[a] |
|---|---|---|---|---|
| 1 | None | 150 | 5 | 14 |
| 2 | 3 | 150 | 5 | 64 |
| 3 | 5 | 150 | 5 | 81 |
| 4 | 10 | 150 | 5 | 91 |
| 5 | 15 | 150 | 5 | 91 |
| 6 | 20 | 150 | 4 | 86 |

*Reaction conditions: benzylamine (0.0085 mol, 0.937 mL), glyoxal (0.0037 mol, 0.427 mL), $CH_3CN$ (7.75 mL), $H_2O$ (0.775 mL), and Ni-Cu-$MgFe_2O_4$ MNPs (10% mol with respect to glyoxal)*

*[a] Isolated yields*

***Table 2: Synthesis of HBIW in the presence of Ni-Cu-$MgFe_2O_4$ MNPs in different solvents.***

| Entry | Solvent | Yield[a] (%) |
|---|---|---|
| 1 | Acetonitrile | 91 |
| 2 | Chloroform | 56 |
| 3 | Ethanol | 61 |
| 4 | Methanol | 71 |
| 5 | Dichloromethane | 53 |

*Reaction conditions: benzylamine (0.0085 mol, 0.937 mL), glyoxal (0.0037 mol, 0.427 mL), solvent (7.75 mL), $H_2O$ (0.775 mL), and Ni-Cu-$MgFe_2O_4$ MNPs (10% mol with respect to glyoxal).*

*[a]Yield of product under ultrasound irradiation (5 min, 150 W).*

***Table 4: Effect of Power ultrasonic irradiation on the synthesis of HBIW.***

| Entry | Power (W) | Time (min) | Yield[a] (%) |
|---|---|---|---|
| 1 | 50 | 5 | 58 |
| 2 | 100 | 5 | 78 |
| 3 | 150 | 5 | 91 |
| 4 | 200 | 5 | 90 |

*Reaction conditions: benzylamine (0.0085 mol, 0.937 mL), glyoxal (0.0037 mol, 0.427 mL), acetonitrile (7.75 mL), $H_2O$ (0.775 mL), and Ni-Cu-$MgFe_2O_4$ MNPs (10 % mol with respect to glyoxal).*

*[a]Yield of product*

the reaction between benzylamine with glyoxal was solvent dependent (Table 2). We found that acetonitrile was the best solvent for this reaction.

### *Influence of reaction time on product yield*

Since the amount of catalyst and solvent were optimized, the influence of reaction time on the reaction was studied in the next step. The effect reaction time on performance HBIW examined and the results are reported in the Table 3.

### *Influence of Ultrasound Power on product yield*

The effect of ultrasonic power inputs from 50 to 200W on the synthesis of HBIW was evaluated (Table 4). The reaction yield increased with the ultrasonic power at 150 W in comparison to 50 and 100 W but decreased at 200 W.

### *Reusability of the Ni-Cu-$MgFe_2O_4$ MNPs*

The catalytic activity and the ability to recycle and reuse Ni-Cu-$MgFe_2O_4$ MNPs were studied in this system.

***Table 5: Reusability and recovery of the Ni-Cu-$MgFe_2O_4$ MNPs catalyst.***

| Run | Yield (%)[a] | Recovery of Ni-Cu-$MgFe_2O_4$ MNPs (%) |
|---|---|---|
| 1 | 91 | 98 |
| 2 | 91 | 98 |
| 3 | 89 | 95 |
| 4 | 87 | 94 |
| 5 | 87 | 94 |

*Reaction conditions: benzylamine (0.0085 mol, 0.937 mL), glyoxal (0.0037 mol, 0.427 mL), acetonitrile (7.75 mL), $H_2O$ (0.775 mL) and Ni-Cu-$MgFe_2O_4$ MNPs (10% mol with respect to glyoxal).*
*[a]Yield of product under ultrasound irradiation (5 min, 150 W).*

***Table 6: Comparison of catalytic activity of Ni-Cu-$MgFe_2O_4$ MNPs with several known catalysts.***

| Entry | Catalyst | Solvent | Conditions | Time (min) | Yield (%)[a] | References |
|---|---|---|---|---|---|---|
| 1 | $CuFe_2O_4$ MNPs | water/acetonitrile | US | 16 | 89 | [34] |
| 2 | $SiO_2$ NPs | water/acetonitrile | US | 5 | 89 | [22] |
| 3 | Citric Acid | water/acetonitrile | US | 5 | 89 | [35] |
| 4 | $H_2SO_4$ | MeOH | 60°C | 540 | 67 | [36] |
| 5 | Chloric(VII) Acid | water/MeOH | 50°C | 360 | 68 | [37] |
| 6 | $BF_3O(C_2H_5)_2$ | Water/EtOH | r.t. | 720 | 67 | [38] |
| 7 | Ni-Cu-$MgFe_2O_4$ MNPs | water/acetonitrile | US | 5 | 91 | This work |

*Reaction conditions: benzylamine (0.0085 mol, 0.937 mL), glyoxal (0.0037 mol, 0.427 mL), acetonitrile (7.75 mL), $H_2O$ (0.775 mL) and Ni-Cu-$MgFe_2O_4$ MNPs (10% mol with respect to glyoxal).*
*[a]Yield of product under ultrasound irradiation (5 min, 150 W).*

After the magnetic separation of catalyst from the reaction mixture, the catalyst was washed with ethanol and dried to remove any remaining ethanol, and reused in the further reactions for several times. The average chemical yield for five consecutive runs was 87%, which clearly demonstrates the practical recyclability of this catalyst (Table 5).

In Table 6, the result obtained from synthesis of HBIW in the presence of Ni-Cu-$MgFe_2O_4$ MNPs has been compared with other catalysts used for this reaction. As can be seen, the catalytic system presented in this paper has advantages in terms of low cost and stable catalyst, short reaction time and excellent yields.

## CONCLUSIONS

In this study, we have reported the green synthesis of $Ni_{0.35}Cu_{0.25}Mg_{0.4}Fe_2O_4$ nanoparticles using tragacanth gel (TG) as a biopolymeric template by the sol-gel method. A single phase with a cubic spinel structure was formed after heat treatment at 700 °C for only 4 h. This method has many advantages such as nontoxic, economic viability, ease to scale up, less time consuming and environmentally friendly approach for the synthesis of Ni-Cu-Mg Ferrite nanoparticles without using any organic chemicals. The catalytic activity of Ni-Cu-Mg Ferrite nanoparticles has been evaluated for the synthesis of HBIW under ultrasonic irradiation. The catalyst is inexpensive and easily available. Moreover, mild reaction conditions, simple procedure, short reaction times, easy workup, high yields of products and ease of separation and recyclability of the catalyst are salient features of the presented work.

**Acknowledgment**

This work is funded by the grant NRF-2015-002423 of the National Research Foundation of Korea.

*Received : Jun. 24, 2018 ; Accepted : Oct. 8, 2018*

**REFERENCES**


[1] Taghavi Fardood S., Ramazani A., Green Synthesis and Characterization of Copper Oxide Nanoparticles Using Coffee Powder Extract, *J. Nanostruct.*, **6**(2): 167-171 (2016).

[2] Saadatjou N., Jafari A., Sahebdelfar S., Synthesis and Characterization of $Ru/Al_2O_3$ Nanocatalyst for Ammonia Synthesis, *Iran. J. Chem. Chem. Eng. (IJCCE)*, **34**(1): 1-9 (2015).

[3] Pouretedal H.R., Basati S., Characterization and Photocatalytic Activity of ZnO, ZnS, ZnO/ZnS, CdO, CdS and CdO/CdS Nanoparticles in Mesoporous SBA-15, *Iran. J. Chem. Chem. Eng. (IJCCE)*, **34**(1): 11-19 (2015).

[4] Taghavi Fardood S., Ramazani A., Joo S.W., Eco-friendly Synthesis of Magnesium Oxide Nanoparticles using Arabic Gum, *J. Appl. Chem. Res.*, **12**(1): 8-15 (2018).

[5] Ramazani A., Taghavi Fardood S., Hosseinzadeh Z., Sadri F., Joo S.W., Green Synthesis of Magnetic Copper Ferrite Nanoparticles using Tragacanth Gum as a Biotemplate and their Catalytic Activity for the Oxidation of Alcohols, *Iran. J. Catal.*, **7**(3): 181-185 (2017).

[6] Alaei M., Rashidi A.M., Bakhtiari I., Preparation of High Surface Area $ZrO_2$ Nanoparticles, *Iran. J. Chem. Chem. Eng. (IJCCE)*, **33**(2): 47-53 (2014).

[7] Alaei M., Mahjoub A.R., Rashidi A., Effect of $WO_3$ Nanoparticles on Congo Red and Rhodamine B Photo Degradation, *Iran. J. Chem. Chem. Eng. (IJCCE)*, **31**(1): 23-29 (2012).

[8] Ramazani A., Ahmadi Y., Fattahi N., Ahankar H., Pakzad M., Aghahosseini H., Rezaei A., Taghavi Fardood S., Joo S.W., Synthesis of 1, 3, 4-Oxadiazoles from the Reaction of N-Isocyaniminotriphenylphosphorane (Nicitpp) with Cyclohexanone, a Primary Amine and an Aromatic Carboxylic Acid *via* Intramolecular Aza-Wittig Reaction of In-Situ Generated Iminophosphoranes, *Phosphorus, Sulfur Silicon Relat. Elem.*, **191**(7): 1057-1062 (2016).

[9] Taghavi Fardood S., Ramazani A., Golfar Z., Joo S.W., Green Synthesis of $\alpha$-$Fe_2O_3$ (hematite) Nanoparticles using Tragacanth Gel, *J. Appl. Chem. Res.*, **11**(3): 19-27 (2017).

[10] Alaei M., Jalali M., Rashidi A., Simple and Economical Method for the Preparation of MgO Nanostructures with Suitable Surface Area, *Iran. J. Chem. Chem. Eng. (IJCCE)*, **33**(1): 21-28 (2014).

[11] Dehno Khalaji A., Solid State Process for Preparation of Nickel Oxide Nanoparticles: Characterization and Optical Study, *Iran. J. Chem. Chem. Eng. (IJCCE)*, **35**(3): 17-20 (2016).

[12] Ahmadi S.H., Davar P., Manbohi A., Adsorptive Removal of Reactive Orange 122 from Aqueous Solutions by Ionic Liquid Coated $Fe_3O_4$ Magnetic Nanoparticles as an Efficient Adsorbent, *Iran. J. Chem. Chem. Eng. (IJCCE)*, **35**(1): 63-73 (2016).

[13] Moradi S., Taghavi Fardood S., Ramazani A., Green Synthesis and Characterization of Magnetic $NiFe_2O_4$@ZnO Nanocomposite and its Application for Photocatalytic Degradation of Organic Dyes, *J. Mater. Sci. Mater. Electron.*, **29**(16): 14151-14160 (2018).

[14] Hassanpour A., Hosseinzadeh-Khanmiri R., Ghorbanpour K., Abolhasani J., Mosaei Oskoei Y., Synthesis of 3,4-Dihydroquinoxalin-2-Amine, Diazepine-Tetrazole and Benzodiazepine-2-Carboxamide Derivatives with the Aid of $H_6P_2W_{18}O_{62}$/Pyridino-$Fe_3O_4$, *Iran. J. Chem. Chem. Eng. (IJCCE)*, **35**(4): 39-47 (2016).

[15] Bayandori Moghaddam A., Hosseini S., Badraghi J., Banaei A., Hybrid Nanocomposite Based on $CoFe_2O_4$ Magnetic Nanoparticles and Polyaniline, *Iran. J. Chem. Chem Eng. (IJCCE)*, **29**(4): 173-179 (2010).

[16] Ramazani A., Farshadi A., Mahyari A., Sadri F., Joo S.W., Asiabi P.A., Taghavi Fardood S., Dayyani N., Ahankar H., Synthesis of Electron-poor N-Vinylimidazole Derivatives Catalyzed by Silica Nanoparticles under Solvent-free Conditions, *Int. J. Nano Dimens.*, **7**(1): 41 (2016).

[17] Khashi M., Allameh S., Beyramabadi S.A., Morsali A., Dastmalchian E., Gharib A., $BiFeO_3$ Magnetic Nanoparticles: A Novel, Efficient and Reusable Magnetic Catalyst for the Synthesis of Polyhydroquinoline Derivatives, *Iran. J. Chem. Chem. Eng. (IJCCE)*, **36**(3): 45-52 (2017).

[18] Lebid M., Omari M., Effects of the Solvent and Calcination Temperature on $LaFeO_3$ Catalysts for Methanol Oxidation, *Iran. J. Chem. Chem. Eng. (IJCCE)*, **35**(3): 75-81 (2016).

[19] Batoo K.M., El-sadek M.-S.A., Electrical and Magnetic Transport Properties of Ni–Cu–Mg Ferrite Nanoparticles Prepared by Sol–Gel Method, *J. Alloys Compd.*, **566**: 112-119 (2013).

[20] Gabal M., Effect of Mg Substitution on the Magnetic Properties of NiCuZn Ferrite Nanoparticles Prepared through a Novel Method using Egg White, *J. Magn. Magn. Mater.*, **321**(19): 3144-3148 (2009).

[21] Shayegan Mehr E., Sorbiun M., Ramazani A., Taghavi Fardood S., Plant-Mediated Synthesis of Zinc Oxide and Copper Oxide Nanoparticles by using Ferulago Angulata (Schlecht) Boiss Extract and Comparison of their Photocatalytic Degradation of Rhodamine B (RhB) under Visible Light Irradiation, *J. Mater. Sci. Mater. Electron.*, **29**(2): 1333-1340 (2018).

[22] Arabian R., Ramazani A., Mohtat B., Azizkhani V., Joo S.W., Rouhani M., A Convenient and Efficient Protocol for the Synthesis of HBIW Catalyzed by Silica Nanoparticles under Ultrasound Irradiation, *J. Energ. Mater.*, **32**(4): 300-305 (2014).

[23] Maksimowski P., Gołofit T., Tomaszewski W., Palladium Catalyst in the HBIW Hydrodebenzylation Reaction. Deactivation and Spent Catalyst Regeneration Procedure, *Cent. Eur. J. Energetic Mater.*, **13**(2): 333-348 (2016).

[24] Nielsen A.T., Chafin A.P., Christian S.L., Moore D.W., Nadler M.P., Nissan R.A., Vanderah D.J., Gilardi R.D., George C.F., Flippen-Anderson J.L., Synthesis of Polyazapolycyclic Caged Polynitramines, *Tetrahedron*, **54**(39): 11793-11812 (1998).

[25] Bellamy A.J., Reductive Debenzylation of Hexabenzylhexaazaisowurtzitane, *Tetrahedron*, **51**(16): 4711-4722 (1995).

[26] Bayat Y., Ebrahimi H., Fotouhi-Far F., Optimization of Reductive Debenzylation of Hexabenzylhexaazaisowurtzitane (the Key Step for Synthesis of HNIW) using Response Surface Methodology, *Org. Process Res. Dev.*, **16**(11): 1733-1738 (2012).

[27] Qiu W., Chen S., Yu Y., The Crystal Structure of Hexabenzoylhexaazaisowurtzitane, *J. Chem. Crystallogr.*, **28**(8): 593-596 (1998).

[28] Crampton M.R., Hamid J., Millar R., Ferguson G., Studies of the Synthesis, Protonation and Decomposition of 2, 4, 6, 8, 10, 12-Hexabenzyl-2, 4, 6, 8, 10, 12-Hexaazatetracyclo [5.5. 0.05, 9.03, 11] Dodecane (HBIW), *J. Chem. Soc., Perkin Trans. 2*, **2**(5): 923-929 (1993).

[29] Taghavi Fardood S., Golfar Z., Ramazani A., Novel Sol–Gel Synthesis and Characterization of Superparamagnetic Magnesium Ferrite Nanoparticles using Tragacanth Gum as a Magnetically Separable Photocatalyst for Degradation of Reactive Blue 21 Dye and Kinetic Study, *J. Mater. Sci. Mater. Electron.*, **28**(22): 17002–17008 (2017).

[30] Zohuriaan M., Shokrolahi F., Thermal Studies on Natural and Modified Gums, *Polym. Test.*, **23**(5): 575-579 (2004).

[31] Ou Y., Jia H., Xu Y., Chen B., Fan G., Liu L., Zheng F., Pan Z., Wang C., Synthesis and Crystal Structure of β-Hexanitrohexaazaisowurtzitane, *Sci. China, Ser. B, Chem.*, **42**(2): 217-224 (1999).

[32] Waldron R., Infrared Spectra of Ferrites, *Phys. Rev.*, **99**(6): 1727-1735 (1955).

[33] Sorbiun M., Shayegan Mehr E., Ramazani A., Taghavi Fardood S., Biosynthesis of Ag, ZnO and Bimetallic Ag/ZnO Alloy Nanoparticles by Aqueous Extract of Oak Fruit Hull (Jaft) and Investigation of Photocatalytic Activity of ZnO and Bimetallic Ag/ZnO for Degradation of Basic Violet 3 Dye, *J. Mater. Sci. Mater. Electron.*, **29**(4): 2806-2814 (2018).

[34] Azizkhani V., Montazeri F., Molashahi E., Ramazani A., Magnetically Recyclable $CuFe_2O_4$ Nanoparticles as an Efficient and Reusable Catalyst for the Green Synthesis of 2, 4, 6, 8, 10, 12-Hexabenzyl-2, 4, 6, 8, 10, 12-hexaazaisowurtzitane as CL-20 Explosive Precursor, *J. Energ. Mater.*, **35**(3): 314-320 (2017).

[35] Shokrollahi S., Ramazani A., Tabatabaei Rezaei S.J., Mashhadi Malekzadeh A., Azimzadeh Asiabi P., Joo S.W., Citric acid as an Efficient and Green Catalyst for the Synthesis of Hexabenzylhexaazaisowurtzitane (HBIW), *Iran. J. Catal.*, **6**(1): 65-68 (2016).

[36] Jefimczyk J., Antczak A., Maksimowski P., Studies on Synthesis of Hexabenzylhexaazaisowurtzitane (HBIW) in the Menthol-Sulfuric Acid System, *Przem. Chem.*, **87**(3): 296-299 (2008).

[37] Gołofit T., Maksimowski P., Szwarc P., Cegłowski T., Jefimczyk J., Scale-Up Synthesis of HBIW, an Intermediate in CL-20 Synthesis, *Org. Process Res. Dev.*, **21**(7): 987-991 (2017).

[38] Bayat Y., Hajighasemali F., An Efficient and Facile Synthesis of CL-20 from TADNO using $HNO_3/N_2O_5$ and Optimization of Reaction Parameters by Taguchi Method, *Propellants, Explosives, Pyrotechnics*, **41**(5): 893-898 (2016).